Int. J. Multiphase Flow, Vol. 7, pp. 151–166, 1981
Printed in Great Britain

0301-9322/81/020151-16$02.00/0
Pergamon/Elsevier

WAVELIKE MOTION OF PARTICULATE SLUGS IN A HORIZONTAL PNEUMATIC PIPELINE

Y. TOMITA, T. JOTAKI and H. HAYASHI
Mechanical Engineering Department, Kyushu Institute of Technology, Kitakyushu 804, Japan

(*Received* 28 *February* 1980; *in revised form* 5 *August* 1980)

Abstract—In the pneumatic transport of polyethylene pellets in the horizontal pipeline, wavelike slugs which resemble solitary waves in an open channel are observed in a settled layer of the particles when a superficial air velocity is smaller than the saltation velocity by Zenz and those transport characteristics such as travelling velocity, length, period of appearance and pressure drop are measured. It is found that the pressure drop by the wavelike slug is estimated by the Ergun equation for the fixed bed.

1. INTRODUCTION

In the pneumatic transport of particulate solids in pipes, it is desired to reduce the transport air velocity as low as possible to minimize power consumption, solids breakage and pipe abrasion. When the air velocity is decreased below some critical value in a dispersed flow region, the transport generally becomes unstable and a pressure drop along the pipe sharply increases, which results in a pipeline blockage in some case. Therefore, it becomes significant to examine the critical air velocity, and many investigations have been made into this problem. Zenz (1964) examined the minimum air velocity, the saltation velocity, required to transport solids without saltation. When the air velocity is further decreased, different flow patterns of gas–solid mixtures appear. Those have been described by Wen & Simons (1959), Welschof (1962), Bohnet (1965), Lippert (1966) and others. However, existing references so far are mainly concerned with the qualitative observation of the flow patterns and seem to lack the quantitative description. A purpose of the present paper is to examine transport characteristics of noncohesive granular solids in a region of low air velocity and to locate those flow patterns in a phase diagram for pneumatic transport in horizontal pipe.

The wavelike motion of particulate slugs is observed when the air velocity is below the saltation velocity, and it is accompanied with a settled layer. The slugs are periodically conveyed to the end of the pipeline, plugging the pipe cross section. But the solid particles in the slug are not the same throughout the slug motion. The solid particles in the settled layer are entrained by the slug when it comes along and are moved over a definite distance by it. When it passes, the particles are left behind in the settled layer. Then, the settled layer is transported downstream as a whole by the same distance every time the slug passes. In this respect movement of solid particles by the slugs looks like that of water particles by solitary waves in an open channel.

As related wavelike phenomena of solid particles there are ripples and dunes which are observed by Wen & Simons (1959). In books by Cornish (1934) and Bagnold (1941) we can find description on the wind-generated ripples and dunes over the bed composed of particles. Similar bed configurations are also observed to occur in river beds and there are many references on this problem: an article by Kennedy (1969) or book by Graf (1971), and so forth. In these cases of bed forms the particles are mainly transported by the action of fluid shear on the bed surface and the fluid flow over the surface has great influence on the transport. On the other hand in the case of wavelike motion of particulate slugs the particles are transported by the action of air flow through the particles.

2. BASIC RELATION

Figure 1 shows a schematic diagram of the wavelike motion of particulate slugs in a pipe, where x is the longitudinal coordinate, p is the pressure, t is the time, H is the height of the settled layer and D is the pipe diameter. The slugs travel with about a constant velocity of c, plugging the

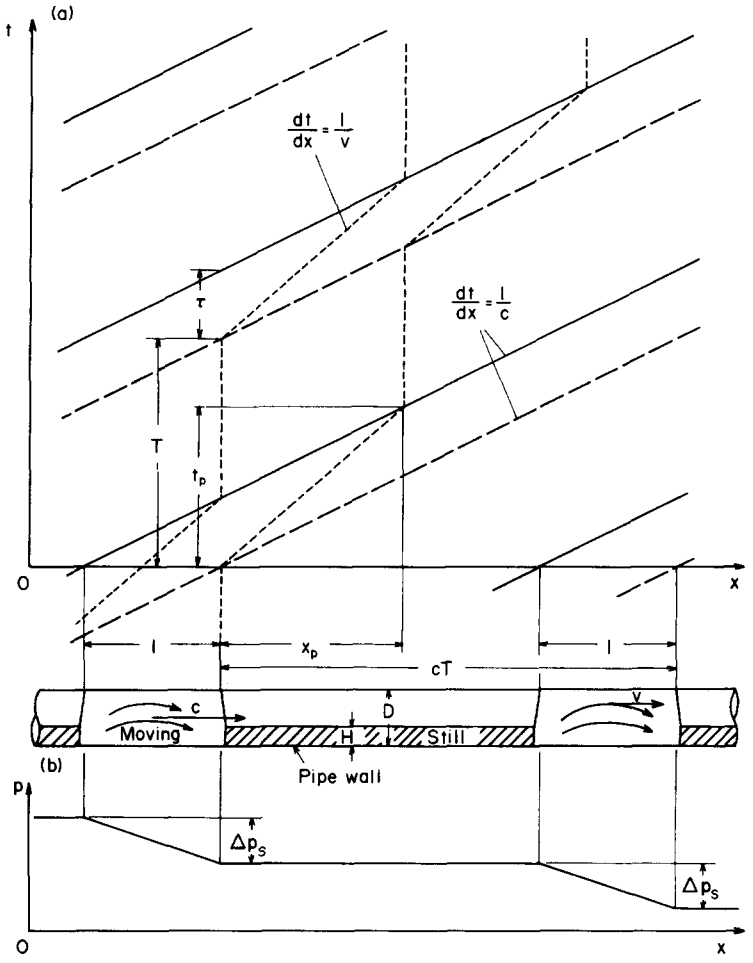

Figure 1. Travelling of particulate slugs; (a) paths of slug and particle:——, path of slug rear; -----, path of slug front; — — —, path of particle; (b) pressure distribution.

pipe cross section. The length of slug, l, is also about constant during its motion. The particles before and behind the slug stand still. When the slug comes along, the particles are accelerated by the slug and are transported over a distance x_p. Then the particles are again still until the next slug comes along. A transit time of slug at a given point, τ, is l/c. In this time the cross section of the settled layer changes from A to A_o over the length of l, where A is the cross-sectional area of the settled layer and A_o is that of the pipe. If we assume that voidage of the slug, ϵ, is equal to that of the settled layer, an average particle's velocity, v, is given by the mass conservation of particles as

$$v = c(A_o - A)/A. \qquad [1]$$

A moving time of the particles by the slug, t_p, is given by

$$t_p = l/(c - v). \qquad [2]$$

Since x_p is vt_p, it relates to l as

$$x_p = l(A_o - A)/A. \qquad [3]$$

If T is the period of the slug appearance and ρ_p is the material density of the particles, a solids mass flow rate, M_p, is given by

$$M_p = A\rho_p(1 - \epsilon)x_p/T = (A_o - A)\rho_p(1 - \epsilon)l/T, \qquad [4]$$

since the particles passing a given point during τ are those in the settled layer of length x_p upstream from that point.

The pressure drop by the slug is Δp_s and that by the pipe friction of air flow is negligibly small.

In the wavelike slug flow, the particles in the settled layer are still. This means that the shear stress at the surface of the settled layer, τ_o, is below the critical value to initiate particle movement, or the fluid threshold (Owen 1964);

$$\tau_o \leqq 0.01 \rho_p g d, \qquad [5]$$

where g is the gravity acceleration and d is the particle diameter. If u_{01} is the average air velocity in particle free cross section above the settled layer and λ is the friction factor of this perimeter for air flow, τ_o is given by

$$\tau_0 = \frac{1}{2} \rho_a u_{01}^2, \qquad [6]$$

where we regard τ_o as an average shear stress over the perimeter. According to the Manning formula λ is given by

$$\lambda = 2gn^2 / r_h^{1/3}, \qquad [7]$$

where r_h is the hydraulic mean depth of the particle free cross section and n is its mean roughness. When H is smaller than $D/2$, n is given in meter and second units as (Tsubaki 1973)

$$n = [\{n_1^{3/2}(1-y^2)^{1/2} + n_2^{3/2}(\pi - \cos^{-1} y)\}/\{(1-y^2)^{1/2} + (\pi - \cos^{-1} y)\}]^{2/3}, \qquad [8]$$

where n is the roughness of the settled surface which is given by $0.04743 d^{1/6}$ (Jaerger 1956), n_2 is that of the pipe wall which is given by 0.009 and y is $(D-2H)/D$. By substituting [6] and [7] for [5] we have

$$u_{01} \leqq T \frac{r_h^{1/6}}{n} (0.01 \rho_p d / \rho_a)^{1/2}. \qquad [9]$$

If u_{02} is the percolating velocity of air through the settled layer, the pressure drop per unit length in the settled layer is given by

$$\frac{\Delta p}{l} = 150 \frac{(1-\epsilon)^2}{\epsilon^2} \frac{\mu u_{02}}{d^2} + 1.75 \frac{(1-\epsilon)}{\epsilon} \frac{\rho_a u_{02}^2}{d}, \qquad [10]$$

where we assume the Ergun equation applicable for it and μ is the dynamic viscosity of air. If this pressure drop is equal to that in the particle free section of the pipe, we have

$$u_{02} = \frac{\sqrt{(gd)}}{\epsilon} \left[\left\{ 1 + \frac{4\beta}{\alpha} \frac{n^2}{r_h^{4/3}(1-\epsilon)} u_{01}^2 \right\}^{1/2} - 1 \right], \qquad [11]$$

where α is $150(1-\epsilon)/\epsilon^3 \rho_a d \sqrt{(gd)}$ and β is $1.75/\epsilon^3$. From the continuity equation for air, we have

$$U = \frac{A - A_o}{A_o} u_{01} + \frac{A}{A_o} \epsilon u_{02}, \qquad [12]$$

where U is the superficial air velocity defined as Q/A_o, Q being the volumetric flow rate of air through the pipe. Thus, if H is specified, we can calculate from [9], [11] and [12] the critical air velocity above which saltation occurs over the settled layer.

3. THE EXPERIMENTAL APPARATUS AND PROCEDURE

Figure 2 shows a schematic diagram of the experimental apparatus. The granular solids in the blow tank are fed into the pipe and transported through it by the compressed air introduced at the upper part of the tank. The i.d. of the tank is 400 mm and its volume is 0.14 m^3. The i.d. of the experimental tube is 42 mm and its length is 11.8 m. The tube is made of transparent plastics except small parts of the inlet and the outlet. To observe the flow patterns in the pipe, the photocells are arranged at intervals of 2 m along the tube. Beams to the photocells are in horizontal direction normal to the tube axis and are arranged so as to cross the upper part of the pipe. The injection feeder is used for returning the transported solids to the blow tank. To avoid external disturbances

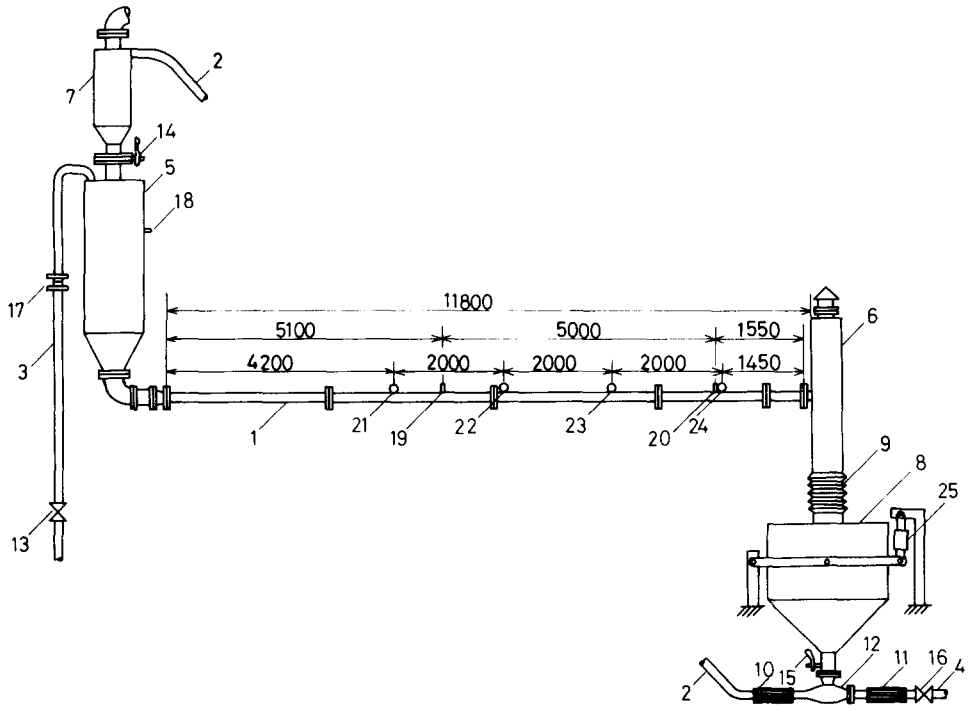

Figure 2. Schematic diagram of experimental apparatus. 1—Experimental tube; 2—return pipe; 3,4—compressed air feeding pipes; 5—blow tank; 6,7—cyclone separators; 8—weighing tank; 9–11—flexible connections; 12—injection feeder; 13—reduced valve; 14—butterfly valve; 15—damper; 16—stop valve; 17—Quadrant flow nozzle; 18–20—pressure pickups; 21–24—photocells; 25—load cell.

during the experiment as far as possible, air which is stored beforehand in air reservoirs is used. Pressure in the tank is kept constant by the reduced valve. The mass flow rate of air is measured by the quadrant flow nozzle and that of solids by the load cell attached to the weighing tank.

The granular solids used in this experiment are spherical polyethylene pellets. The mean diameter is 3.09 mm, the material density is 920 kg/m^3 and the bulk density is 589 kg/m^3. According to calculation, the free falling velocity of a single particle is 8.38 m/s and the minimum fluidizing velocity is 0.613 m/s for $\epsilon = 0.35$ and 0.782 m/s for $\epsilon = 0.40$. The minimum air velocity, the single-particle saltation velocity by Zenz (1964), U_s, is 4.7 m/s.

The travelling velocity of the slug is given by

$$c = \Delta l/\Delta t, \qquad [13]$$

where Δt is the time lag obtained from the output signals of two photocells which are Δl apart. The length of slug is given by

$$l = c\tau, \qquad [14]$$

where τ is obtained from the output signal for single photocells. The number of slugs in the experimental tube, N, is given by

$$N = L/cT, \qquad [15]$$

where T is obtained from the output signals of single photocells and L is the tube length. In the following data, c is determined by the third and the fourth photocells from the upstream side and T and τ are by the fourth photocell.

The superficial air velocity at the pipe inlet, U_t, is given by

$$U_t = (M_a - M_p\rho_{at}/\rho_a)/A_o\rho_{at}, \qquad [16]$$

where ρ_{at} is the air density in the tank and M_a is the mass flow rate of air measured by the quadrant flow nozzle. The superficial air velocity U in [12] is given by $U_t\rho_{at}/\rho_a$, where ρ_a is the air density determined by the mean pressure across the slug. There was a unique relation between U and U_t.

4. EXPERIMENTAL RESULTS AND DISCUSSION

4.1 *Phase diagram*

Figure 3 shows the mass flow rate of solids and the solid loading ratio m vs U_t, where m is defined as $M_p/A_o\rho_a U$. It is seen that the transport starts when U_t is near 1 m/s. This value is considerably smaller than the saltation velocity by Zenz. For blow tanks of which conveying pipe stands up vertically and goes out from the upper part of the tank, it is necessary for U_t to be larger than the free falling velocity of a single particle. Furthermore, it is seen that transport density of solids is considerably high in comparison with that in the dispersed flow.

Figure 4 shows the phase diagram for pneumatic transport in horizontal pipe, where the pressure drop per unit length is plotted against the superficial air velocity in the pipe. In the slug flow, the pressure distribution in the pipeline is not steady since the pressure drop is almost due to the moving slugs. However, if the pressure is averaged over a long time, the pressure drop per unit length is given by $\Delta p_t/L$, where Δp_t is the gauge pressure at the tank and the pipe end is open to the atmosphere in this experiment. In the figure, the pressure drops by air flow through the empty pipe, through the fixed bed and through the pipe with a settled layer. The last ones are calculated by [10], [11] and [12] for a given H. The relation between H and U is given in figure 5. Furthermore, for reference, the pressure drops for the dispersed flow of about equal particles to those of this experiment are plotted, which are estimated by the measurements in pipes of 54.0, 81.1, 105.3 and 130.0 mm dia. (Tomita *et al.* 1978). The wavelike slug flow is observed when U is smaller than about 6 m/s above which the settled layer disappears. This velocity is near U_s. Lippert (1966) gave a similar diagram to figure 4 with

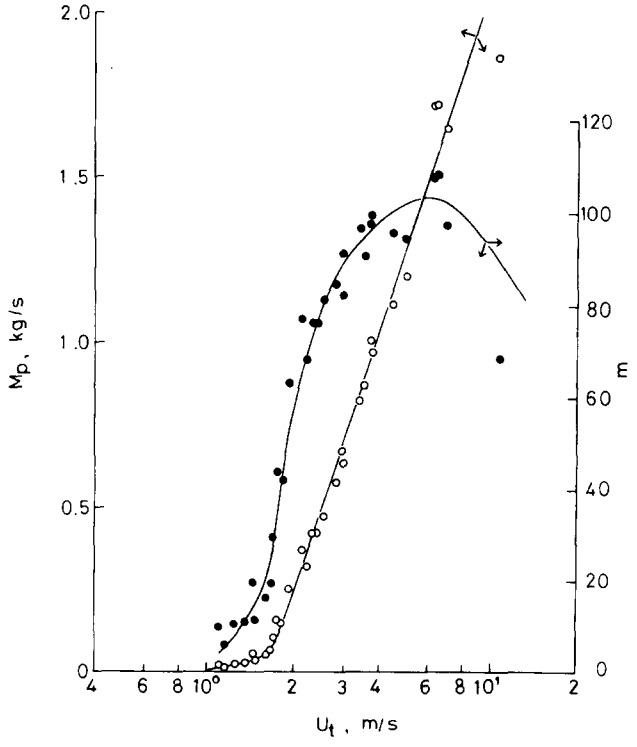

Figure 3. Mass flow rate of solids and solid loading ratio.

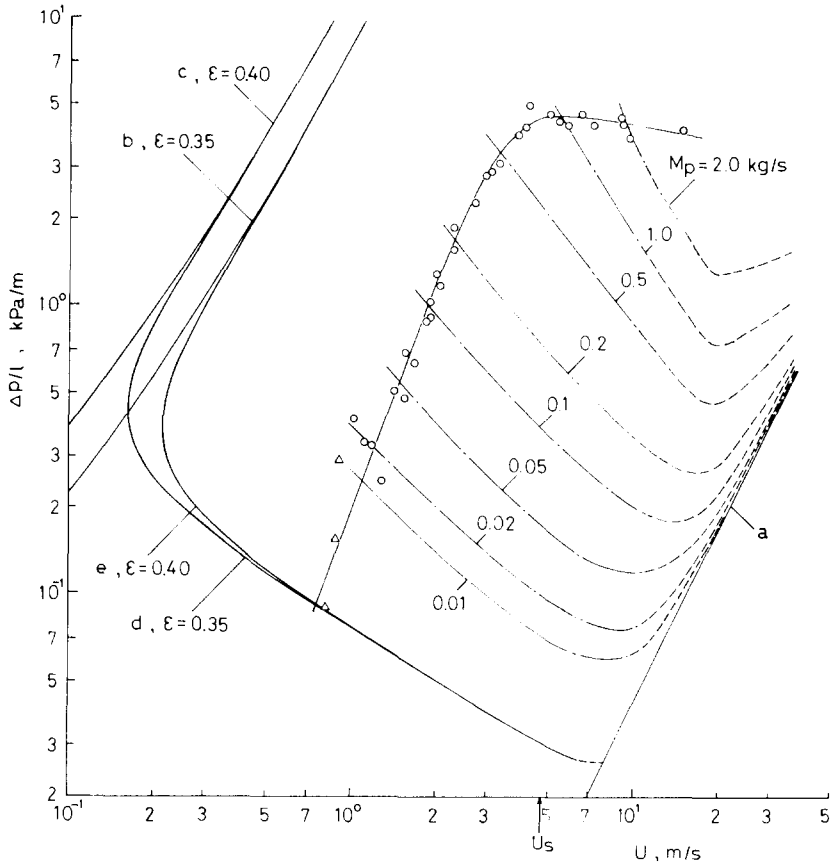

Figure 4. Phase diagram for pneumatic transport in horizontal pipe; ○, $M_p \neq 0$, Δ, $M_p = 0$; -----, dispersed flow; a, air flow through the empty pipe; b,c, air flow through the fixed bed; d,e, air flow through the pipe with a settled layer.

M_p as a parameter. But he did not observe the wavelike slug flow. The reason why the present experimental data are obtained only along a line in the phase diagram is that the mass flow rate of solids is uniquely determined by U_t in the present type of blow tank (Jotaki & Tomita 1978). If we could make an experiment in other points in the phase diagram, we might be able to observe such flow patterns with the dunes and the ripples which are observed by Wen & Simons (1959), although it cannot be said positively since the particle size and pipe diameter are different from those in this experiment.

4.2 *Flow pattern of the wavelike slug flow*

When Δp_t is small enough the particles do not appear at the pipe inlet. When Δp_t is arranged to give rise to the slug flow, the particles enter the pipe in saltation and stops to form a settled layer after a definite flight. Succeeding particles travel in saltation over the settled layer and make it higher and longer. When the length of the layer increases, say about 1 m, and the free space above it becomes narrower, it suddenly rises to plug the pipe cross section and particles feeding from the tank stop. Then, the front part of the layer, say about 40 cm, separates and begins to move plugging the pipe. Figure 5 shows this process. There remains a lower settled layer behind the moving slug since the velocity of particles is smaller than that of slug. The slug, however, soon collapses and stops because there are no particles in front of the slug and because the slug leaves the particles behind. Since the tank pressure is kept constant, the velocity of air consequently increases and the particle feeding starts again, where M_a is kept constant. Thus, the above-mentioned process is repeated and the length of settled layer increases. The

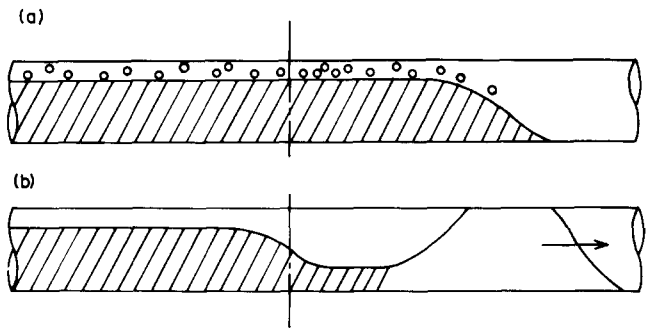

Figure 5. Slug formation at the beginning of transport near the pipe inlet; (a) particles feeding in saltation before separation, (b) slug movement after separation; the chain lines show a separation position.

net transport of particles begins only after the front part of the settled layer arrives at the pipe end. Then, it is said that a new slug is formed when another slug is going out from the pipeline. In the present experiment, it was not observed that the particles travelled in saltation over the entire length of pipeline. We noticed that when the present particles were transported in the dispersed flow region in steel pipes the particles were considerably charged. However, in this experiment the velocity of particles is small enough and we regard that the particles are not charged strongly. Even if the particles are charged, it does not seem that the electrostatic force has great influence upon the wavelike slug flow since the particle size is relatively large.

Figure 6 shows the photographs of the slug. With increasing air velocity the slug front is disturbed more and more, and the slope of the slug rear becomes steep. To observe the particles motion by the slug a known height of settled layer was arranged in advance where the color of particles was changed alternately as shown in figure 7(a). Then, the tank pressure was arranged to give rise to the wavelike slug flow corresponding to this height of settled layer. Figure 7(b) shows that all the particles in the slug are moved, being replaced with those in the settled layer. It is inferred from figure 7(c) that the particles moving in the upper part is faster than those moving in the lower part. This was found by Hayano *et al.* (1976) in case of transport of rape seed in rectangular pipe, although they described that the slug slid on the settled layer. But in this case the settled layer is moved downstream by a definite length when the slug passes. In this respect, the motion of solid particles by the slug is analogous to that of water particles by solitary waves in an open channel.

4.3 *Characteristics of the slugs*

Figure 8 shows the relation between U and the height of settled layer, where the solid line is the critical air velocity, above which saltation occurs over the settled layer, calculated by [9]–[12] assuming $\epsilon = 0.35$. The data support this calculation and, indeed, there was no saltation before and behind the slug.

Figure 9 shows the travelling velocity of slug vs U. The ranges of data show the standard deviations, although the number of data is not the same: it is about in proportion to U. Figure 10 shows the period of the slug appearance vs U. Figure 11 shows the number of slugs in the pipeline vs U, where in evaluation of N by [15] we use each average values for c and T. When U is smaller than 1.6 m/s, N is about unity and about 4 when U is larger than 2 m/s. According to the mechanism of slug formation, it is inferred that N is integer, which seems to be confirmed approximately. Thus, it follows that in the above two regions of U, T is in inverse proportion to U since c is approximately in proportion to U.

Figure 12 shows τ vs U. When U is about 1.4 m/s, τ takes a maximum. Thus, it is expected that l takes extreme values. This is shown in figure 13, where the experimental points of l by [14] are averages of the product of c by τ. The ranges are the standard deviations for this l.

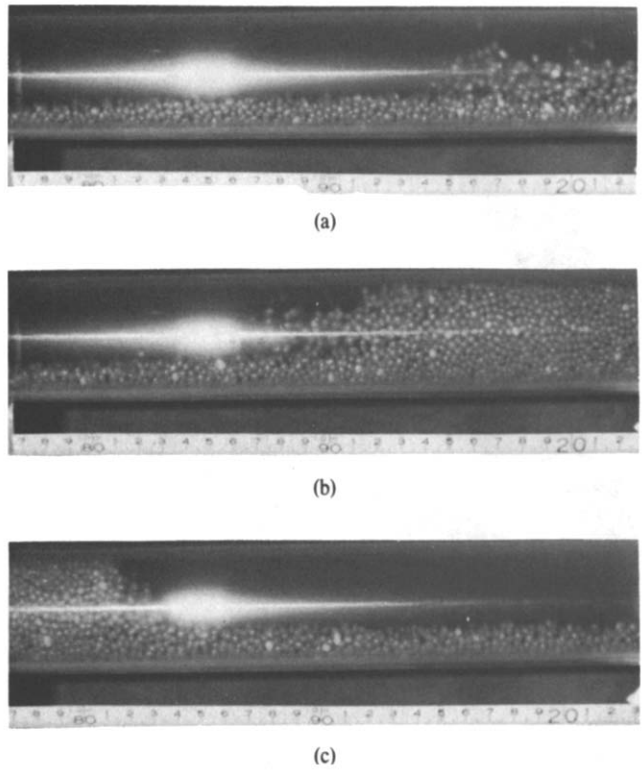

Figure 6. Successive photographs showing how the wavelike slug passes through the pipe when U is about 2.4 m/s; (a) settled layer before slug arrival, (b) slug front, (c) slug rear.

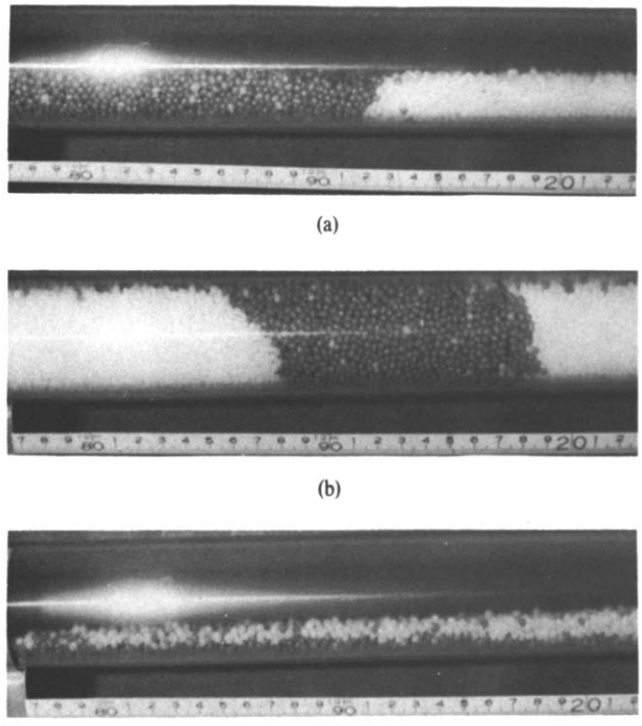

Figure 7. Successive photographs showing how the solid particles are transported by the wavelike slug when U is about 1.2 m/s; (a) Settled layer before slug arrival, (b) solid particles in the slug, (c) settled layer after the slug passing.

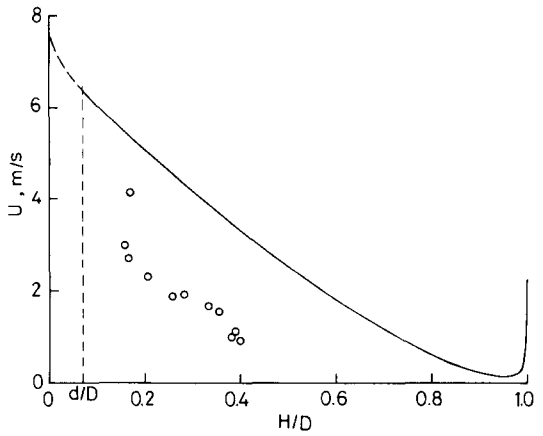

Figure 8. Superficial air velocity versus height of a settled layer in the wavelike slug flow region; the solid line shows the critical air velocity above which saltation occurs over the settled layer of a given height of H.

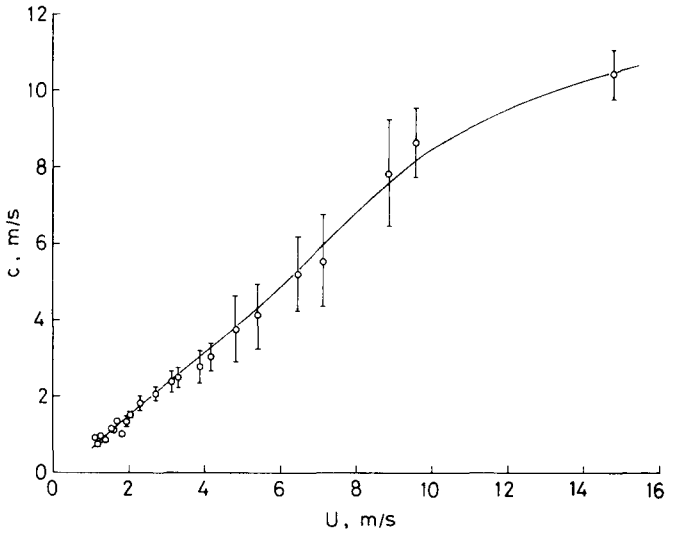

Figure 9. Slug velocity.

As above-mentioned, the slug is formed during a time when another slug goes out from the pipeline. This time is τ. The velocity of particles which enter the pipe in saltation is in proportion to U_t. Then the slug length is in proportion to $U_t\tau$. In figure 13, $U_t\tau$ is plotted. Correlation between l and $U_t\tau$ is high. From [4], l can be also evaluated by M_p, A and T. This can be used as a partial test of the slug flow model. In figure 13 these lengths are plotted assuming $\epsilon = 0.35$. The calculation is limited for U below 6 m/s since A cannot be estimated precisely above it. It is seen that the model holds when U is smaller than 2 m/s. For larger values of U, there frequently appeared incomplete slugs which had only a short plugging part despite the substantially long slugs. Thus, it seems that the photocells measured smaller τ which resulted in smaller length of l by [14]. This is one reason why discrepancy between the model and the measurements increases for larger values of U. Furthermore, it should be noted that the average voidage of the slugs possibly increases with U. The same thing is to be said about M_p; i.e. M_p by [4] becomes smaller than the measurements when U is larger than 2 m/s.

Figure 14 shows x_p by [4] vs U. For larger U than 2 m/s, x_p is larger than cT since cT is about 3 m in this range. When U is 5.4 m/s, x_p becomes L. This means that the particles at $x = 0$ are transported to the pipe end by one slug.

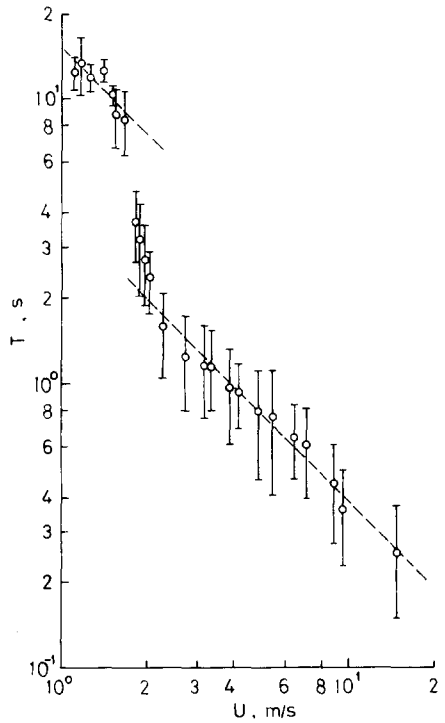

Figure 10. Period of slug appearance; the dashed lines show $T \propto U^{-1}$.

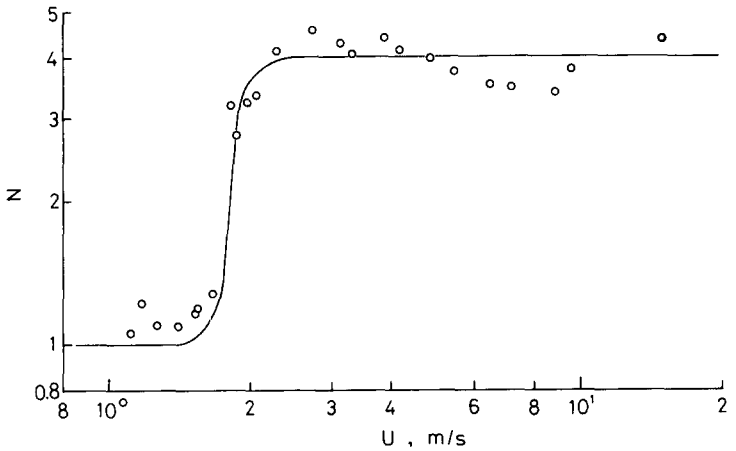

Figure 11. Number of the slug in the experimental tube.

Figure 15 shows Δp_s vs U. When U is smaller than 6 m/s, Δp_s is in proportion to U. If we can omit the pressure drop by the pipe friction of air flow, the overall pressure drop Δp_t will be equal to $N\Delta p_s$. Figure 16 shows $N\Delta p_s$ vs Δp_t. In the wavelike slug flow region Δp_t agrees to $N\Delta p_s$. When U is larger, $N\Delta p_s$ underestimates Δp_t. If we take account of the result in figure 15, this means that the pressure drop in spaces between slugs cannot be omitted. It was also shown that the pressure drop per unit length by the slug, $\Delta p_s/l$, traces a similar trend to that of Δp_s for a change of U. If we assume that $\Delta p_s/l$ can be estimated by the Ergun equation for the fixed bed, it is given by [10], where we substitute $(U - v)/\epsilon$ for u_{02}. Figure 17 shows the relation between $\Delta p_s/l$ and $U - v$, where v is given by [1] and $\Delta p_s/l$ is the average of quotient of Δp_s by l. The calculations are limited in the wavelike slug flow region. It is said that the pressure drop by the slug is estimated by the Ergun equation, although there is a considerable spread in the data.

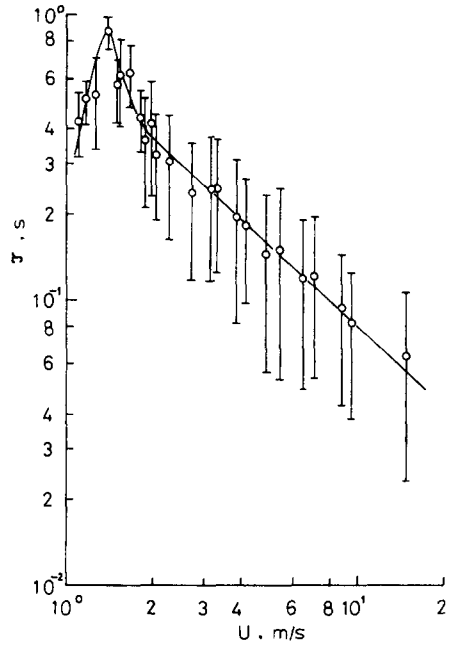

Figure 12. Transit time of the slug.

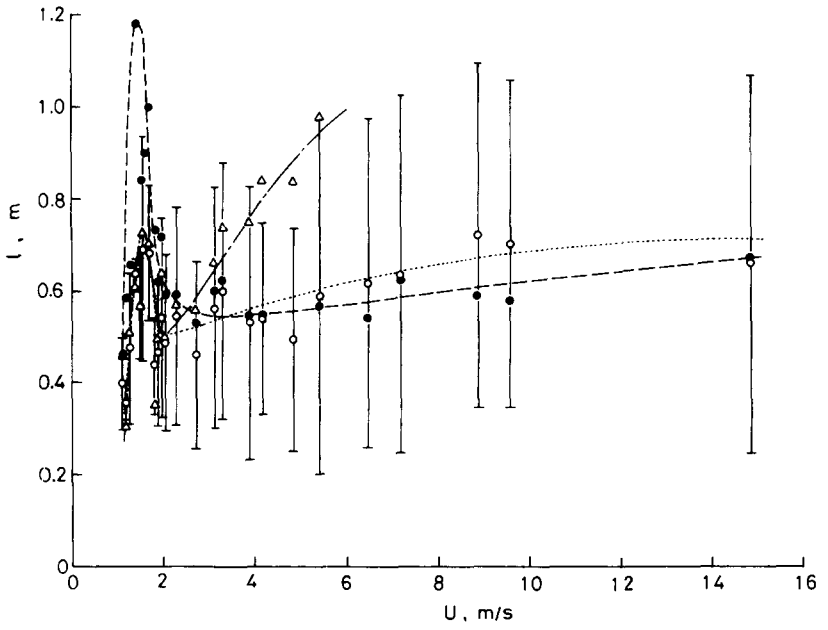

Figure 13. Length of the slug; O, experimental points by[14]; Δ, calculated values by [4]; ●, shows $U_t\tau$.

The driving force for the slug motion is Δp_s and there is a frictional force acting opposite direction to Δp_s which is due to the slug weight and due to the material pressure. If we assume that the average material pressure acting normal to the pipe wall is given by $k\Delta p_s$. The frictional force due to the latter is $fk\Delta p_s \pi Dl$, where k is a constant dependent on the particles and f is the static frictional factor between solid particles and pipe wall. Tsunakawa *et al.* (1979) assumed it as $fk\Delta p_s A_o$. To initiate slug movement the following inequality should hold;

$$A_o \Delta p_s \geqq f\{k\Delta p_s \pi Dl + A_o \rho_p g(1-\epsilon)l\}. \quad [17]$$

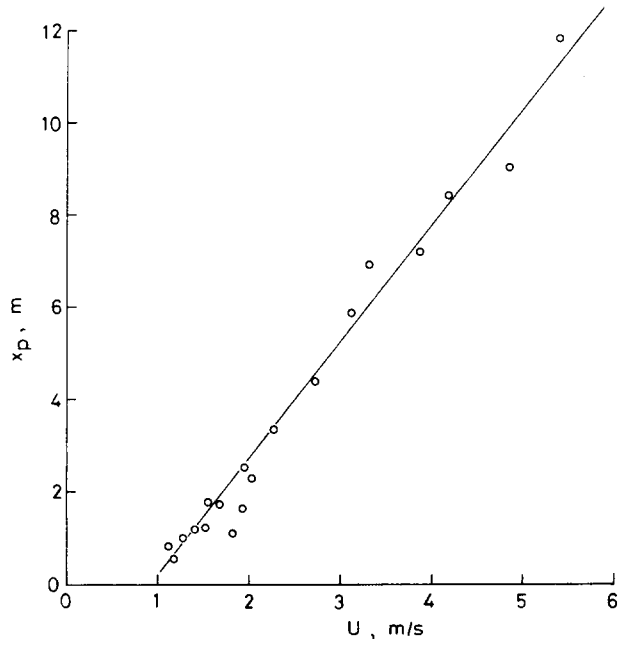

Figure 14. Transported length of the solid particles by the slug.

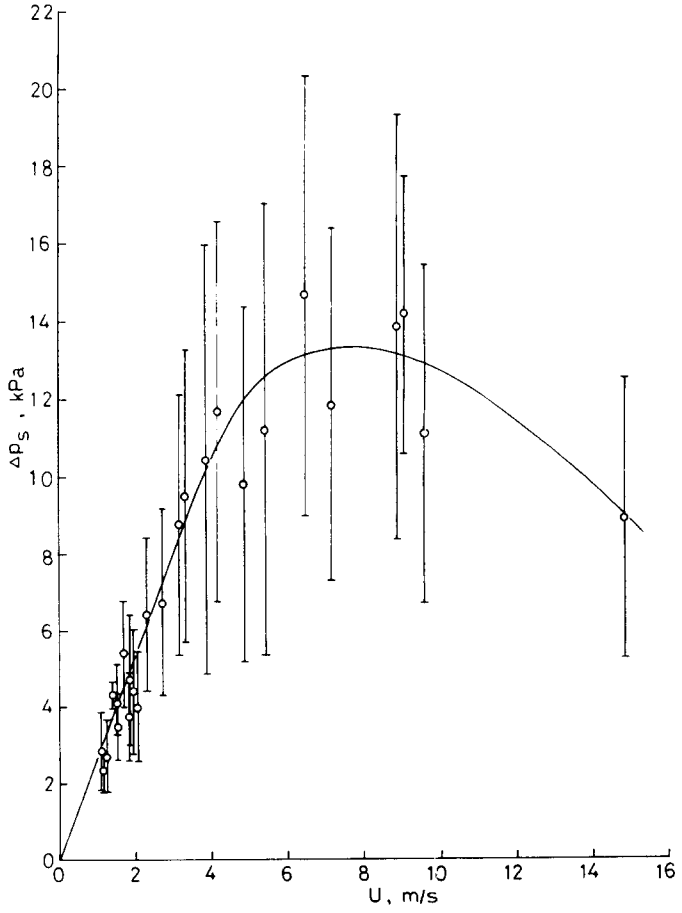

Figure 15. Pressure drop by the slug.

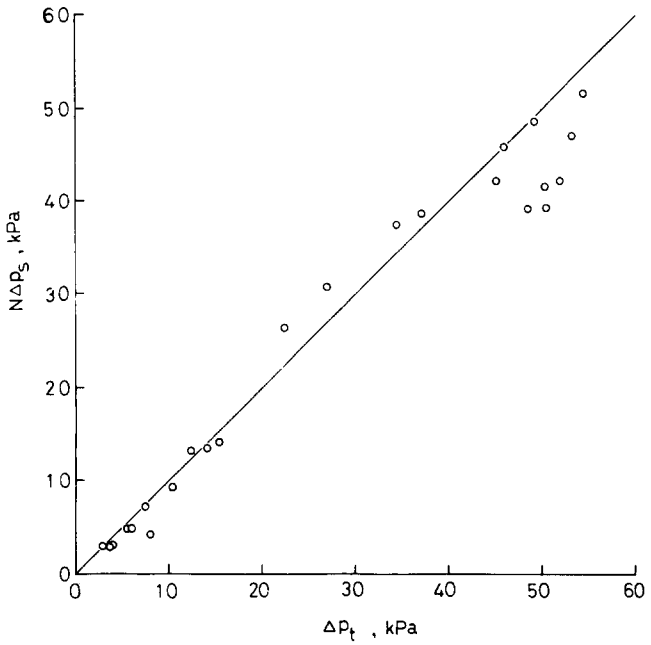

Figure 16. Overall pressure drop vs total pressure drop by the slugs; the solid line is $\Delta p_t = N\Delta p_s$.

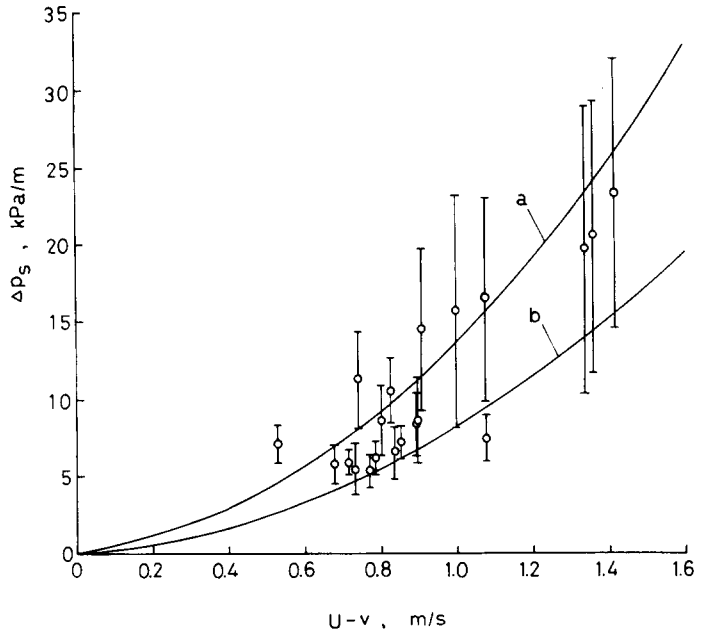

Figure 17. Pressure drop per unit length in the slug vs relative air velocity to the solid particles; the solid lines show the Ergun equation for the fixed bed; a, $\epsilon = 0.35$, *b*, $\epsilon = 0.40$.

From [17] we have

$$l \leqq \frac{D\Delta p_s}{f\{4k\Delta p_s + \rho_p g(1-\epsilon)D\}}. \qquad [18]$$

Figure 18 shows l vs Δp_s. If we fit [18] to the data obtained in a region of U below 2 m/s taking account of the result in figure 13, we have $f = 0.62$ and $k = 0.017$ for $\epsilon = 0.35$. By these values we have 0.996 m as an asymptotic value of l when Δp_s tends to infinity in [18]. Thus result shows

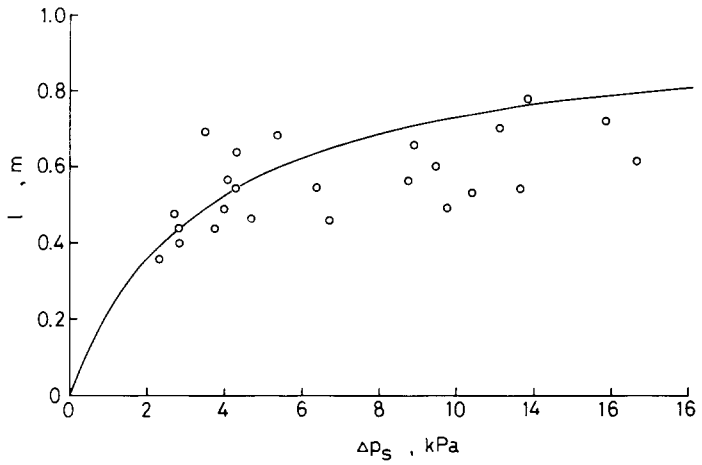

Figure 18. Slug length vs pressure drop by the slug; the solid line is calculated by [18] for $\epsilon = 0.35$, $f = 0.62$ and $k = 0.017$.

that the smaller the slug length is, the smaller the pressure drop is. Lippert (1966) obtained a similar relation to this result for the plug flow without a settled layer.

5. CONCLUSION

In this work we have examined the pneumatic transport of noncohesive granular solids in a region of lower air velocity below the dispersed flow region. Our data were obtained only along a line in the phase diagram for pneumatic transport due to the feed rate characteristics of the present type of blow tank. Thus, it follows that the present work depicts a cross-sectional view of the phase diagram cut along that line. The wavelike slug flow appears when the air velocity is lower than the single-particle saltation velocity by Zenz. The pressure drop by the wavelike slug is found to be estimated by the Ergun equation for the fixed bed. It does not seem that plugging the pipe cross section by the particles is essential to the wavelike slug flow. We observed the wavelike slug flow without plugging the pipe cross section when U is larger.

Acknowledgement—We wish to thank Mr. Y. Hakuno for his cooperation in this work.

NOMENCLATURE

A cross-sectional area of a settled layer
A_o pipe cross-sectional area
c travelling velocity of the slug
D pipe diameter
d particle diameter
f static frictional factor between solid particles and pipe wall
g acceleration due to gravity
H height of a settled layer
k constant dependent on the particles
l length of the slug
M_a mass flow rate of air
M_p mass flow rate of solids
m solid loading ratio

N number of the slug in the pipeline
n mean roughness of the particle free cross section
n_1 roughness of the surface of a settled layer
n_2 roughness of the pipe wall
p pressure
Δp_s pressure drop by the slug
Δp_t pressure at the tank
Q volumetric flow rate of air
r_h hydraulic mean depth of particle free cross section
T period of the slug appearance
t time
t_p moving time of particles by the slug
U superficial air velocity in the pipe
U_s single-particle saltation saltation velocity by Zenz
U_t superficial air velocity at the pipe inlet
u_{01} average air velocity in particle free cross section above the settled layer
u_{02} percolating air velocity through the settled layer
v particle velocity
x longitudinal coordinates
x_p transported length of particles by the slug
y $(D-2H)/D$
α $150\mu(1-\epsilon)/\epsilon^3\rho_a d\sqrt{(gd)}$
β $1.75/\epsilon^3$
ϵ voidage
λ pipe friction factor for air
μ dynamic viscosity of air
ρ_a density of air
ρ_{at} density of air in the tank
ρ_p material density of paricle
τ transit time of the slug
τ_o shear stress at the surface of the settled layer

REFERENCES

BAGNOLD, R. A. 1941 *The Physics of Blown Sands and Desert Dunes.* Methuen, London.

BOHNET, M. 1965 Experimentalle und theoretische Untersuchungen über das Absetzen, das Aufwirbeln und den Transport feiner Staubteilchen in pneumatischen Förderleitungen. VDI-Forsch. -Heft 507.

CORNISH, V. 1934 *Ocean Waves and Kindred Geophysical Phenomena and Additional Notes by H. Jeffreys.* Cambridge University Press.

GRAF, W. H. 1971 *Hydraulics of Sediment Transport.* McGraw-Hill, New York.

HAYANO, N., HARADA, N., WATANABE, H. & JOTAKI, T. 1976 High density, low velocity pneumatic conveying of the fragile materials—II. *Yamaguchi-daigaku Kogakubu Kenkyuhokoku* **27**, 117–125 (in Japanese).

JAEGER, C. 1956 *Engineering Fluid Mechanics*, p. 30. Blakie, London.

JOTAKI, T. & TOMITA, Y. 1978 Characteristics of a blow tank solids conveyor and its operating points working on pipe lines. *Proc. 4th Int. Conf. Pneumatic Transport of Solids in Pipes, BHRA Fluid Engng* 1 D4–51.

KENNEDY, J. F. 1969 The formation of sediment ripples, dunes, and antidunes. *Ann. Rev. Fluid Mechanics* **1**, 147–168 (Edited by W. R. SEARS and M. VAN DYKE). Annual Reviews Inc., Palo Alto.

LIPPERT, A. 1966 Pneumatische Förderung bei hohen Gutkonzentrationen. *Chemie-Ing.-Tech.* **38**, 350–355.

OWEN, P. R. 1964 Saltation of uniform grains in air. *J. Fluid Mech.* **20**, 225–242.

TOMITA, Y., JOTAKI, T. & INOUE, M. 1978 Horizontal pneumatic transport of granules at optimal operation condition. *J. Soc. Powder Tech., Japan* **15**, 389–394 (in Japanese).

TSUBAKI, T. 1973 *Suirigaku*, p. 147. Morikita, Tokyo (in Japanese).

TSUMAKAWA, H., NAKAI, J. & AOKI, R. 1979 Pneumatic conveying of solid plugs. *J. Soc. Powder Tech., Japan* **16**, 249–254 (in Japanese).

WELSCHOF, G. 1962 Pneumatische Förderung bei groβen Fördergutkonzentrationen. VDI-Forsch.-Heft 492.

WEN, C. Y. & SIMONS, H. P. 1959 Flow characteristics in horizontal fluidized solids transport. *AIChE J.* **5**, 263–267.

ZENZ, F. A. 1964 Conveyability of materials of mixed particle size. *I&EC Fund.* **3**, 65–75.